Peer-reviewed version available at Metals 2018, 8, 926; doi:10.3390/met8110926

The impact of Pt concentration on crystal growth mechanism in Pt-Pd binary alloy system in the context of molecular Dynamics

Servet Kızılagac[1]
Physics Department, Science Institute,
[1]Bitlis Eren University, 13000, Bitlis, Turkey
Fatih Ahmet Celik[2] and Koray Koksal[2]
Physics Department, Faculty of Arts and Sciences,
[2,]Bitlis Eren University, 13000, Bitlis, Turkey*

Abstract

This work aims to investigate the effect of Pt concentration on crystal growth mechanism of Platinum-Palladium (Pt-Pd) binary alloy system during the annealing process starting from amorphous phase until some definite temperatures. The calculations have been performed by using molecular dynamic (MD) simulations. Interatomic interactions are described by on Sutton-Chen type Embedded Atom Potential Energy function. In order to understand the main structural properties at the stable and unstable phases, changes in RDF curves versus time have been analysed for different annealing temperatures. Crystalline type bonded pairs have been determined using MD calculations which is required for the computation of Avrami coefficients and for understanding crystal growth mechanism. The results demonstrate that the increase in concentration of Pt during annealing leads to migration of atoms in the crystal lattice points, elimination of dislocations and formation of perfect crystal structure.

Key Words: Molecular Dynamics, Crystal Growth, Avrami coefficients, Pt-Pd Alloy

*Corresponding author. Tel :+90 (434) 222 0000 Fax: +90 (434) 222 0101
E-mail address: facelik@beu.edu.tr

1. Introduction

Platinum (Pt) is a heavy, malleable and grayish white coloured used in significant technological applications. In the last decade, a large amount of studies has been introduced on platinum and platinum-based alloys. Pt-Pd, Pt-Ni and Pt-Rh can be given as examples of this kind of alloys [1–3]. Although Pt and Pt-based alloys are costly materials, they are commonly-used in industry and technology due to their unique physical properties [4]. Particularly, these metal alloys are preferred for some applications areas such as electronics, crystal growth, automotive, semiconductor technology and jewellery industry [5]. Furthermore, pure platinum is served as a material in energy, medicine and space because of high melting temperature. It has also resistance against corrosive effects in room temperature. All these properties make Pt and Pt-based materials attractive in technology [6].

Rhodium and Palladium are suitable elements for solid solution because they are easily soluble in Platinum. Platinum based Palladium solid solutions are forgeable and have some important physical properties [7, 8]. Particularly, Pt-Pd alloys are used in the productions of thin films and play an important role in experimental studies of metallurgical science. Despite their advantages, many physical properties of Pt-alloys have not been determined, since Pt is rare in nature and expensive. Furthermore, experimental investigation of nanoscale behaviour of Pt is not practical [9]. There is a paucity of contribution on physical mechanisms such as phase transitions and magnetic properties of nanoscale clusters of Pd-alloys [10]. Atomic groups in clusters have different physical properties compared with that of bulk structure. Some difficulties arise during the experimental studies, because these atomic groups can be transformed into different structures and groups within a short period of time. This type of difficulties can be eliminated by strong simulations which are prefered in different disciplines [11–13].

One of the most important developments in computer technology is the increasing capability of simulation and modelling which are very significant for nearly all scientific studies [14]. As an example, computer programming underlies studies on genetic science. Recently, in the fields such as nanotechnology, crystal growth and cluster physics, interest in simulation applications has been increased depending on increasing computer power and facilities [15]. Especially, molecular dynamics (MD) simulation has become one of the most important methods in recent years [16– 18]. It describes the molecular systems by imitating the behaviour of atoms and molecules at the microscopic level. At the same time, molecular calculations are able to obtain the physical properties of the model systems under different conditions, such as crystallization from amorphous phase during annealing process [19, 20].

In this current study, we aim to obtain crystallization properties of Pt-Pd alloy at certain annealing temperatures for different Pt concentrations. We investigate whether the volume fraction is influenced by atomic clusters containing crystal-type bonded pairs (which are determined by Honeycutt-Andersen Method (HA)) during phase transitions. In our calculations, geometry and volume dependent Parrinello and Rahman (PR) MD has been used. The parameters of potential energy function (PEF) based on Sutton-Chen family of potential have been fitted to the experimental parameters of alloy and validity limit has been tested. The Avrami exponents have been calculated by using volume fraction to understand the crystallization mechanism at different annealing temperatures during the amorphous phase.

Preprints (www.preprints.org) | NOT PEER-REVIEWED | Posted: 18 October 2018 doi:10.20944/preprints201810.0409.v1

Peer-reviewed version available at Metals 2018, 8, 926; doi:10.3390/met8110926

2. Theory

2.1. Molecular Dynamic Simulation

Molecular dynamic (MD) simulation method aims to obtain some physical properties of the system by using a programming language which perform a sequence of numeric calculations and which includes interactions between the atoms forming the system [21]. In this method, the system is described by interaction forces between atoms which are located on lattice points in a cubic structure MD cell. Equilibrium state and minimum energy condition is provided by using a potential energy function [22]. In our calculations, change of volume and shape with periodic conditions in MD cell are regarded, which has been improved by Parrinello and Rahman (PR) [23]. A typical MD simulation is performed in three steps which are preparation, stabilization, getting results and analysis. In the first step, initial speeds are assigned according to the well-known Maxwell-Boltzman distribution function and atoms are located in lattice points regarding crystal structure of suggested material. During the second step, equation of motion of atoms in the system is obtained by using some numerical integration algorithms and atoms are directed to the point which has minimum energy in phase space. In the last stage, some measurements and analyses are performed on the system in equilibrium [24].

In PR MD method, edge vectors of calculated cell are represented by three time dependent vectors **A**(t), **B**(t) and **C**(t). A cell matrix is defined as **h**(t) = (**ABC**) and Lagrange function of the cell with changeable volume and geometry can be written as

$$L_{PR} = \frac{1}{2}\sum_{i=1}^{N} m_i(\dot{s}_i^t \mathbf{G} \dot{s}_i) - \Phi(r) + \frac{1}{2}W \quad \mathrm{Tr}(\mathbf{h}^{\cdot}\ t\mathbf{h}^{\cdot}) - pd11\Omega \qquad (1)$$

which equation can be used to derive following equations of motion

Preprints (www.preprints.org) | NOT PEER-REVIEWED | Posted: 18 October 2018 doi:10.20944/preprints201810.0409.v1

Peer-reviewed version available at Metals 2018, 8, 926; doi:10.3390/met8110926

$$\ddot{\mathbf{s}}_i = -\sum_{j\neq i}^{N} m_i^{-1} \frac{d\phi(r_{ij})}{r_{ij} dr_{ij}} (\mathbf{s}_i - \mathbf{s}_j) - \mathbf{G}^{-1}\dot{\mathbf{G}}\dot{\mathbf{s}}_i \tag{2}$$

$$\mathbf{h}^{\cdot\cdot} = W^{-1}(\mathbf{\Pi} - \mathbf{I}p)\sigma \tag{3}$$

where **Π** describe the microscopic stress tensor coming from virial theorem and **I** is unit matrix. $\varphi(r_{ij})$ indicates the potential energy function which represents physical interactions between *i* and *j* atoms [25].

In this study, we have used MD simulation method put forward by PR for NPT and we have examined model alloy system at constant pressure. The molecular dynamics step has been set up 5.01 fs and equations of motions have been integrated by a fifth-order Gear predictor-corrector algorithm. The model system with 4000 atoms built in super-lattice structure of Pt-Pd alloy at different concentration of Pt, Pt_xPd_{100-x} (x=50, 70, 90). The system has been constructed $L1_0$ lattice at Pt_{50}-Pd_{50}, and $L1_2$ at Pt_{70}-Pd_{30}, finally FCC lattice at Pt_{90}-Pd_{10} crystal structures. During the MD calculations, firstly, the systems are heated above melting points which are known as experimentally for different concentration values of Pt. Then, the systems are rapidly cooled up to 300 K at the cooling rate of 1×10^{13} *K/s* to observe amorphous phase. Finally, the systems are again heated starting from amorphous phase during annealing.

2.2. Embedded Atom Method (EAM)

According to this method, total energy of a crystal is

$$E_T = \varepsilon \sum_{i=1}^{N} \left[\frac{1}{2} \sum_{j\neq i}^{N} \left(\frac{a}{r_{ij}} \right)^n - c\sqrt{\bar{\rho}_i} \right]$$

Preprints (www.preprints.org) | NOT PEER-REVIEWED | Posted: 18 October 2018 doi:10.20944/preprints201810.0409.v1

Peer-reviewed version available at Metals 2018, 8, 926; doi:10.3390/met8110926

where first term, φ_{ij} shows two body interaction potential between i and j atoms. Second term, $F_i(\rho_i)$ indicates embedding functional depending on charge density [26], ρ_i, which reads

$$\overline{\rho}_i = \sum_{j \neq i}^{N} \left(\frac{a}{r_{ij}} \right)^m$$

The potential energy parameters between atoms are obtained in the studies [5, 27].

The radial distribution function (RDF) is calculated to understand the structural features of model system at solid-liquid-amorphous phase transitions. The mathematical expression of RDF, $g(r)$, as following

$$g(r) = \frac{V}{N^2} \frac{\sum_i n_i(r)}{4\pi r^2 \Delta r}$$

where r is the radial distance, $n_i(r)$ is the coordination number of atom i separated with r within Δr interval and brackets denote the time average [22].

2.3. Honeycutt-Andersen Method (HA)

Studies on atomic clusters show that this method is very important to obtain some physical properties such as crystallization from amorphous phase, solid-solid phase transitions, crystal growth. An experimental investigation of microscopic structure and behaviors in different conditions is very tough for atomic clusters having little number $(2 - 7)$ of neighbour atoms. Structural analysis of this kind of clusters which arise during the phase transitions is possible by performing a method developed by Honeycutt and Anderson [28]. According to HA method, in a cluster atomic arrange or atomic structure is described by four basic indices ($ijkl$) as seen in Fig. 1. The value of i is 1 if two atoms make a bond and i will be 2 in the case of non-bonded pair. Second indice, j represents the number of neighbor atoms shared by both of the pair atoms. Third

Peer-reviewed version available at Metals 2018, 8, 926; doi:10.3390/met8110926

indice, k is number of bonds between neighbor atoms. l is distinctive indice which represents the difference in bond geometry in the structure. For example, 1421 and 1422 represent the bond pairs which are forming characteristic FCC and HCP structures, respectively [28, 29]. 1551, 1541 and 1431 are used to determine the ideal and defected ICOS structures, respectively. These are most basic bond pairs representing the amorphous structure. 1661 and 1441 are basic pairs of BCC lattice structure. The existence of bond formation is ensured by cut-off distance which corresponds to the region between first and second peaks in RDF [30].

2.4. Johnson-Mehl-Avrami (JMA) Crystallization Kinetics

Parameters such as Avrami coefficients and crystallization properties of a material can be calculated by using the results obtained from experimental measurements. Crystallization kinetics are developed by JMA and improved by different researchers. JMA equation for fixed temperature crystallization kinetics reads [31]

$$-ln(1-x) = (k\,t)^n \tag{7}$$

where x is volume-fraction which varies in t period, n is Avrami exponent and k is reaction velocity of growth and nucleation. This equation can be written as

$$ln[-ln(1-x)] = n\,ln(k) + n\,ln(t) \tag{8}$$

Here, the variation in volume fraction which means the gradient of the plot of the function $ln[-ln(1-x)]$ according to $ln(t)$ gives Avrami exponent. Experimental studies result that Avrami exponential (n) can take the values between 1 − 4. The case of n = 1 refers to surface nucleation

and one-dimensional growth, $n = 2$ refers volume nucleation and one-dimensional growth, $n = 3$ refers to volume nucleation and two-dimensional growth, $n = 4$ is volume nucleation and three dimensional growth [32, 33]. The percentage of bonded pairs such as 1421, 1441, 1661 and 1422 which are the basis of the crystal unit cell atomic clusters formed during the annealing process from amorphous phase of modelled system is determined depending on structural transitions. During the isothermal crystallization, the volume fraction depending on variation of percentage will be calculated for different annealing temperatures. Avrami exponents will be obtained using this fraction in Eq. 8.

3. Results and Discussions

JMA kinetics is one of the most efficient techniques which are used to determine crystallization properties and kinetics of a material. Information about Avrami exponent leads to understand the crystallization mechanism during annealing process starting amorphous phase at 300 K [34]. In order to obtain Avrami exponents, the number of bonded pairs has been investigated during the annealing process. Here, bonded pairs represent the crystal structure and they are determined by HA-method-based MD calculations. In addition, it has been proposed that Avrami coefficient in JMA equations can be obtained by using percentage variation of crystalline pairs which can be considered as a function of volume fraction, X.

For three different Pt concentrations of Pt-Pd system, Fig. 2 shows the change of the number of crystal bonded pairs which are obtained by increasing the temperature from 300 K (amorphous phase) to 400 − 700 K. At 800 K, system has transformed into liquid phase for all Pt concentrations. The total number of crystalline bonded crystal pairs which represent FCC, BCC and HCP crystal lattices has been calculated by HA method (1421 + 1422 + 1441 + 1661). The

Peer-reviewed version available at Metals 2018, 8, 926; doi:10.3390/met8110926

number of crystal bonded pairs is lower for $Pt_{50}Pd_{50}$ which means that system is not completely transformed to stable crystal phase at the temperature of 400 K. Increase in annealing temperature leads to the increase in total number of crystalline bonded pairs for all the Pt concentrations at 800 K. Furthermore, addition of Pt atoms to the system increases the number of crystalline-type bonded pairs. Particularly, the amount of bonded pairs is found as 70% of $Pt_{90}Pd_{10}$ during the annealing process.

Radial distribution function (RDF) has been applied to reveal the atomic distribution along the distance between described central atom and neighbouring atoms [35]. For a gaseous system, the number of atoms in a definite volume is small because of the motion of atoms and distribution of atoms is independent from *r* distance. This situation is different for a solid material due to less atomic vibrations and motion so that atoms form a close-packed structure. Therefore, the peaks of RDF curves have been observed for some definite atomic distances. In amorphous systems, there is a peak at the distance between the most neighboring atoms and the central atom which shows high probability of existence of the atoms at this distance. The atomic density of second and third neighboring atoms have been indicated by other peaks which are obscure. The increase in the number of the peaks point out stability of average density for remote atomic distance.

Figs. 3 and 4 show RDF curves which are obtained in a certain time and for different Pt concentrations of Pt-Pd systems. In this annealing process, the temperature is increased from 300 K (amorphous phase) to 400 and 700 K. At an annealing temperature of 400 K, crystal phase transition has not been observed for Pt_{50}-Pd_{50} system which is stabilized in amorphous phase in which case atoms become completely disordered. Second peak (corresponds to amorphous phase) of RDF curves are splitted. This is because of high cooling speed so that atoms cannot find an opportunity to be located in lattice points and they are randomly distributed in MD cell. In another word, atoms are distributed arbitrarily in MD cell because high cooling rate prevents the required time for location of atoms in crystal lattice points. The intensity of crystal peaks is obviously

increasing with the increase in Pt concentration. This is the result of the formation of more stable crystal lattice structure. Increase in the number of Pt atoms leads to the location of atoms in lattice points. Same situation is valid for annealing temperature of 700 K. Rising the annealing temperature causes an increase in the strength of the peaks for all Pt concentrations. As seen from the Figs. 3 and 4 for annealing time of 0.750 ns and for Pt_{90}-Pd_{10}, the intensity of second and third peaks of RDF in the case of 400 K are weaker compared with that of 700 K. This result has a good agreement with the change of the number of crystal bonded pairs shown in Fig 2.

Here, an another investigation about the effect of bonded pairs on growth process enables us to determine the existence probability of bonded pairs in the system and percentage change is used for obtaining Avrami exponents in JMA equations. Percentage variation of crystalline-type bonded pairs in the range between initial and final growing time has been taken into account to determine the Avrami coefficients. Obtained curve gives the Avrami coefficients when the change of $ln(-ln(1-x))$ (here x corresponds to the percentage variation of crystalline bonded pairs) according to $ln(t)$ has been fitted. Figs. 7(a), 7(b) and 7(c) indicate the fitting curves for different Pt concentrations of Pt-Pd system at 400 and 700 K temperatures. These curves give the Avrami coefficients or exponents (n). Avrami coefficient value for $Pt_{50}Pd_{50}$ is 0.48 at 400 K and 1.43 at 700 K. In $Pt_{70}Pd_{30}$ system, Avrami coefficients for 400 K and 700 K are 1.25 and 1.96, respectively. Avrami value is 2.3 for $Pt_{90}Pd_{10}$ at 400 K and 3.68 at 700 K. Avrami coefficients are increasing with the annealing temperature for all the concentrations which means that surface and one-dimensional nucleation is effective for low temperature and three dimensional nucleation is observed for higher annealing temperature. The concentration is also effective on the coefficients.

Avrami coefficients provide a convenient information to understand the crystal growth mechanism in a certain temperature [36]. In phase transitions, nucleation and crystal growth mechanisms are extremely important [37, 38]. For two different annealing temperature values, the

change in Avrami exponents with Pt concentrations has been shown in Fig. 8. It can be clearly seen from this figure that the values of Avrami exponents increase with increasing of Pt concentrations. Besides, while the annealing temperature increase, the values of Avrami exponents increase for different Pt concentrations. Particularly, the value of *n* is approaching to 4 at 700 K for $Pt_{90}Pd_{10}$. This result indicates that three dimensional growth take place as a result of increase in Pt.

Fig. 7(a) shows the image of atomic distribution of Pt_{50}-Pd_{50} for 400 K annealing temperature. In this figure, there is no crystal layers and the structure seems as amorphous. Fig. 7(b) and 7(c) are images of atomic distributions from different point of view for Pt_{90}-Pd_{10}. The atoms start to be located into the crystal lattice points with the increase of Pt and atomic layers can be clearly seen from the figure. This image is consistent with the figures related to Avrami coefficients. Fig. 8 shows the atomic distribution of Pt_{90}-Pd_{10} alloy for an annealing temperature of 700 K. The Figs. 7 and 8 indicate that an increase in Pt concentration leads to definite atomic arrays and the structure is transformed into the crystal structure. At this annealing temperature, Avrami coefficient is determined as nearly 4 which is a sign of three dimensional growths.

4. Conclusions

In this study, our main goal is to investigate and reveal the effect of Pt concentration on crystal growth mechanism for Pt-Pd binary alloy system using molecular dynamics simulation. For this purpose, we consider that the experimentally obtained volume fraction is corresponding to the variation of percentage of crystal-type bonded pairs which is representing nano-size atomic clusters and is required to calculate Avrami coefficients during the annealing process. For different annealing temperatures (from amorphous to crystal phase) of chosen model alloy system, it has been calculated and concluded that the values of Avrami coefficients increase with Pt

concentration. The value of Avrami coefficient is about 4 at an annealing temperature 700 K, which shows that the crystal growth occurs at three dimension. For Pt_{90}-Pd_{10} alloy, $700K$ has been determined as an ideal annealing temperature value in which temperature it is possible to observe perfect crystallization process.

5. References

[1] Z. M. Rdzawski, J. P. Stobrawa, Microstructure and properties of the new pt–rh based alloys for hightemperature applications, Journal of materials processing technology 153 (2004) 681–687.

[2] D. Ren, J. Qin, J. Wang, T. T. Tsong, Oscillatory compositional depth profiles in surface segregation of a pt-rh alloy, Physical Review B 47 (7) (1993) 3944.

[3] J. P. Clay, J. P. Greeley, F. H. Ribeiro, W. N. Delgass, W. F. Schneider, Dft comparison of intrinsic wgs kinetics over pd and pt, Journal of Catalysis 320 (2014) 106–117.

[4] W. Wang, Z. Wang, J. Wang, C.-J. Zhong, C.-J. Liu, Highly active and stable pt–pd alloy catalysts synthesized by room-temperature electron reduction for oxygen reduction reaction, Advanced Science 4 (4).

[5] J. Luyten, J. De Keyzer, P. Wollants, C. Creemers, Construction of modified embedded atom method potentials for the study of the bulk phase behaviour in binary pt–rh, pt–pd, pd–rh and ternary pt–pd–rh alloys, Calphad 33 (2) (2009) 370–376.

[6] F. A. Celik, The investigation of nucleation rate and johnson–mehl–avrami model of pt–pd alloy using molecular dynamics simulation during heat treatment processes, Journal of Alloys and Compounds 632 (2015) 116–121.

[7] G. Shao, J. Zhangr, T. Li, Investigation of potential parameters effect on stable structures of pt-pd alloy nanoparticles by particle swarm algorithm, in: Automation (YAC), 2017 32nd Youth Academic Annual Conference of Chinese Association of, IEEE, 2017, pp. 316–320.

[8] H. Garbacz, J. Mizera, Z. Laskowski, M. Gierej, Microstructure and mechanical properties of a pt–rh alloy produced by powder metallurgy and subjected to plastic working, Powder technology 208 (2) (2011) 488–490.

[9] K. Yuge, A. Seko, A. Kuwabara, F. Oba, I. Tanaka, First-principles study of bulk ordering and surface segregation in pt-rh binary alloys, Physical Review B 74 (17) (2006) 174202.

[10] E. Sosa, H. Liu, Oxygen adsorption on pt-pd nanoclusters by dft and ab initio atomistic thermodynamics, Journal of Alloys and Compounds 735 (2018) 643–653.

[11] H. Tanaka, Relationship among glass-forming ability, fragility, and short-range bond ordering of liquids, Journal of non-crystalline solids 351 (8-9) (2005) 678–690.

[12] U. Gasser, A. Schofield, D. Weitz, Local order in a supercooled colloidal fluid observed by confocal microscopy, Journal of Physics: Condensed Matter 15 (1) (2002) S375.

[13] C. Desgranges, J. Delhommelle, Molecular simulation of the nucleation and growth of gold nanoparticles, The Journal of Physical Chemistry C 113 (9) (2009) 3607–3611.

[14] M. Celtek, S. Sengul, The characterisation of atomic structure and glass-forming ability of the zr– cu–co metallic glasses studied by molecular dynamics simulations, Philosophical Magazine (2018) 1–20.

[15] Z. Liu, R. Zhang, Aacsd: An atomistic analyzer for crystal structure and defects, Computer Physics Communications 222 (2018) 229–239.

[16] S. Ozgen, E. Duruk, Molecular dynamics simulation of solidification kinetics of aluminium using sutton–chen version of eam, Materials Letters 58 (6) (2004) 1071–1075.

[17] A. Yildiz, F. Celik, Atomic concentration effect on thermal properties during solidification of pt-rh alloy: A molecular dynamics simulation, Journal of Crystal Growth 463 (2017) 194–200.

[18] Y. Zhang, S. Jiang, Atomistic mechanisms for temperature-induced crystallization of amorphous copper based on molecular dynamics simulation, Computational Materials Science 151 (2018) 25–33.

[19] X. Zhu, K. Chen, Molecular dynamics simulation of homogeneous nucleation of kbr cluster, Journal of Physics and Chemistry of Solids 66 (10) (2005) 1732–1738.

[20] W. Yu, X.-x. WANG, H.-l. WANG, Atomic simulation on evolution of nano-crystallizaion in amorphous metals, Transactions of Nonferrous Metals Society of China 16 (2006) s327–s331.

[21] S. Kazanc, S. Ozgen, O. Adiguzel, Pressure effects on martensitic transformation under quenching process in a molecular dynamics model of nial alloy, Physica B: Condensed Matter 334 (3-4) (2003) 375–381.

[22] S. Kazanc, Molecular dynamics study of pressure effect on crystallization behaviour of amorphous cuni alloy during isothermal annealing, Physics Letters A 365 (5-6) (2007) 473–477.

[23] M. Parrinello, A. Rahman, Crystal structure and pair potentials: A molecular-dynamics study, Physical

Review Letters 45 (14) (1980) 1196.

[24] J. M. Haile, Molecular dynamics simulation: elementary methods, Vol. 1, Wiley New York, 1992.

[25] D. C. Rapaport, D. C. R. Rapaport, The art of molecular dynamics simulation, Cambridge university press, 2004.

[26] A. Sutton, J. Chen, Long-range finnis–sinclair potentials, Philosophical Magazine Letters 61 (3) (1990) 139–146.

[27] G. Dereli, T. Cagin, M. Uludogan, M. Tomak, Thermal and mechanical properties of pt-rh alloys, Philosophical magazine letters 75 (4) (1997) 209–218.

[28] J. D. Honeycutt, H. C. Andersen, Molecular dynamics study of melting and freezing of small lennardjones clusters, Journal of Physical Chemistry 91 (19) (1987) 4950–4963.

[29] L. Wang, H. Liu, K. Chen, Z. Hu, The local orientational orders and structures of liquid and amorphous metals au and ni during rapid solidification, Physica B: Condensed Matter 239 (3-4) (1997) 267–273.

[30] N. Jakse, A. Pasturel, Ab initio molecular dynamics simulations of local structure of supercooled ni, The Journal of chemical physics 120 (13) (2004) 6124–6127.

[31] J. William, R. Mehl, Reaction kinetics in processes of nucleation and growth, Transactions of the Metallurgical Society of AIME 135 (1939) 416–442.

[32] M. Avrami, Kinetics of phase change. i general theory, The Journal of Chemical Physics 7 (12) (1939) 1103–1112.

[33] X. Li, M. Yan, J. Wang, H. Huang, C. Kong, G. Schaffer, M. Qian, Non-isothermal crystallization kinetics and mechanical properties of al86ni6y4. 5co2la1. 5 metallic glass powder, Journal of Alloys and Compounds 530 (2012) 127–131.

[34] X. Xie, H. Gao, Calorimetric studies on the crystallization of li2s–b2o3 glasses1, Journal of noncrystalline solids 240 (1-3) (1998) 166–176.

[35] Y. Qi, T. C¸agın, Y. Kimura, W. A. Goddard III, Molecular-dynamics simulations of glass formation and crystallization in binary liquid metals: Cu-ag and cu-ni, Physical review B 59 (5) (1999) 3527.

[36] P. Zhang, W. Hui, Y. Zhang, X. Ren, D. Zhang, Molecular dynamics simulation for the rapid solidification process of mgo–al2o3–sio2 glass–ceramics, Journal of Non-Crystalline Solids 358 (12-13) (2012) 1465–1473.

[37] K. Lu, Nanocrystalline metals crystallized from amorphous solids: nanocrystallization, structure, and properties, Materials Science and Engineering: R: Reports 16 (4) (1996) 161–221.

[38] F. A. C¸elik, S. Kazanc, A. Yildiz, S. Ozgen, Pressure effect on the structural properties of amorphous ag during isothermal annealing, Intermetallics 16 (6) (2008) 793–800.

FIGURES

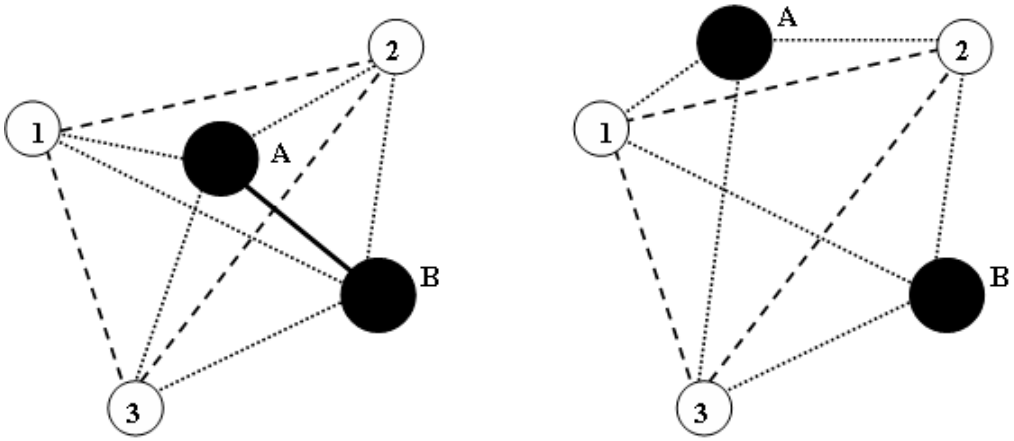

FIG. 1. Representation of Honeycutt-Anderson method. Continuous line shows root pair which makes a bond with each other. Dotted line indicates the neighbor atoms which make bond with root pair. Dashed line represents the bonds between neighbor atoms. (left) 1331 bonded pair and (right) 2331 non-bonded pair.

Preprints (www.preprints.org) | NOT PEER-REVIEWED | Posted: 18 October 2018 doi:10.20944/preprints201810.0409.v1

Peer-reviewed version available at Metals 2018, 8, 926; doi:10.3390/met8110926

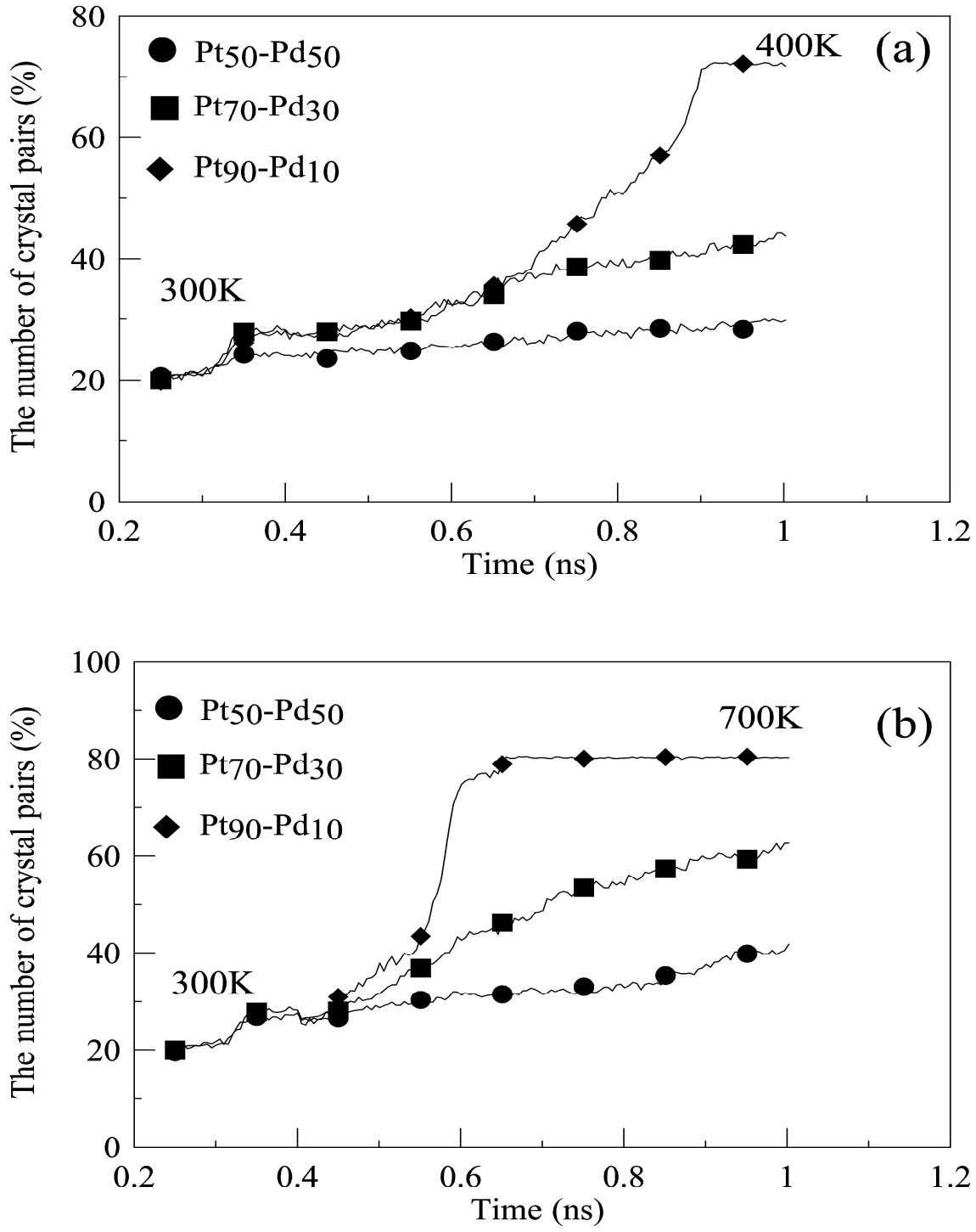

FIG. 2. The variation of the number of crystal bonded pairs with time for different Pt concentration rates in Pt-Pd alloy during annealing.

Preprints (www.preprints.org) | NOT PEER-REVIEWED | Posted: 18 October 2018 doi:10.20944/preprints201810.0409.v1

Peer-reviewed version available at Metals 2018, 8, 926; doi:10.3390/met8110926

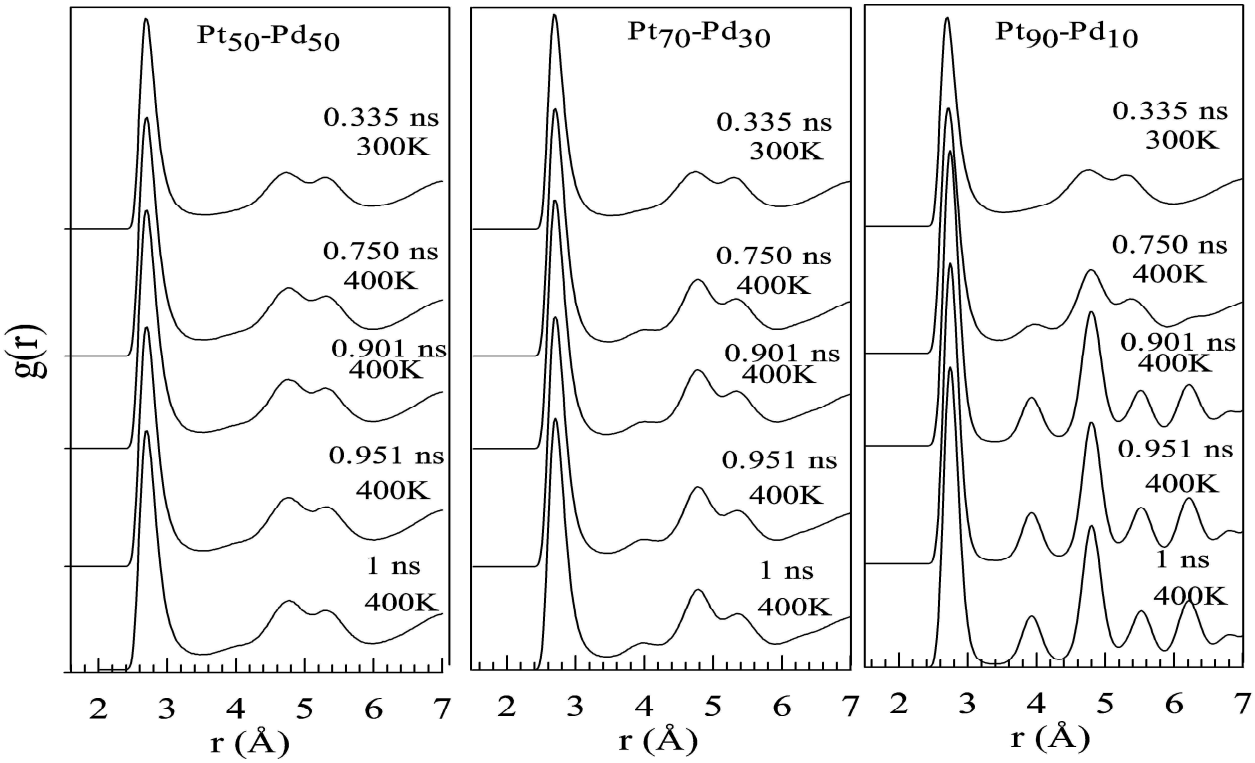

FIG. 3. RDF curves obtained at different times and for different temperatures of the process 300 and 400 K.

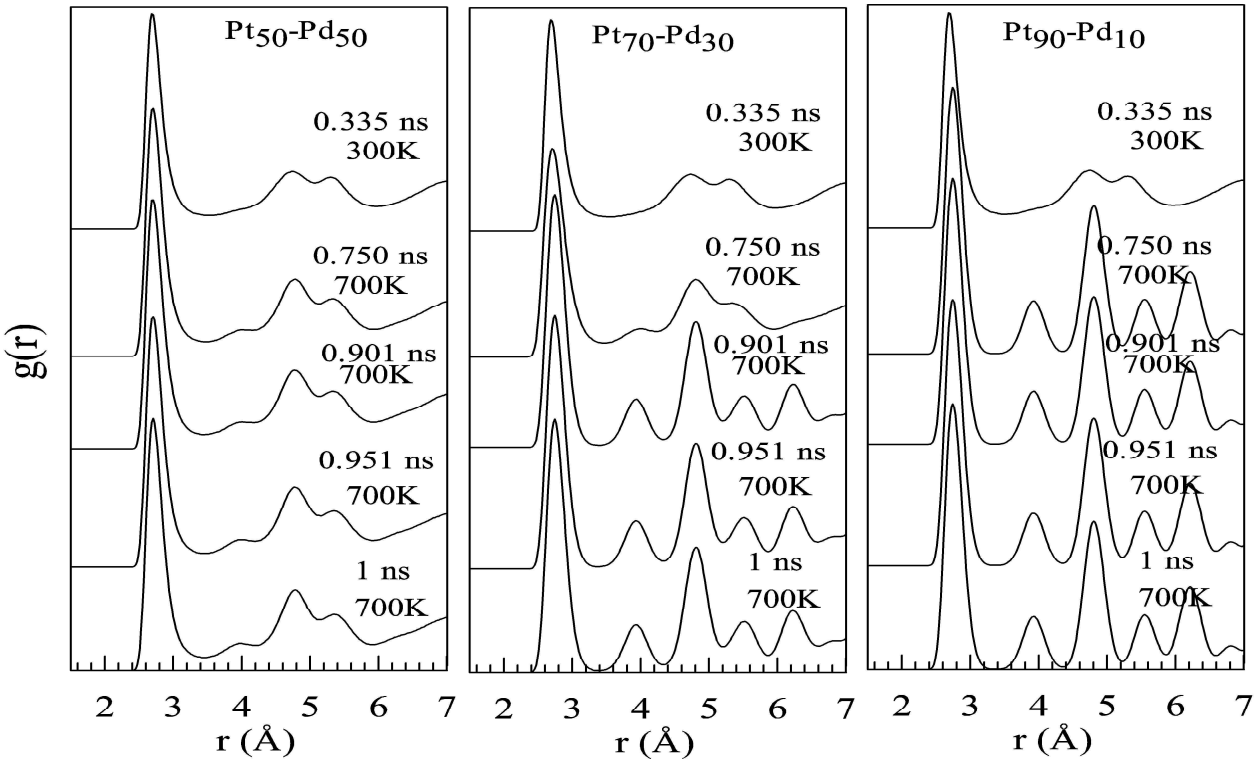

FIG. 4. RDF curves obtained at different times and for different temperatures of the process 300 and 700 K.

Preprints (www.preprints.org) | NOT PEER-REVIEWED | Posted: 18 October 2018 doi:10.20944/preprints201810.0409.v1

Peer-reviewed version available at Metals 2018, 8, 926; doi:10.3390/met8110926

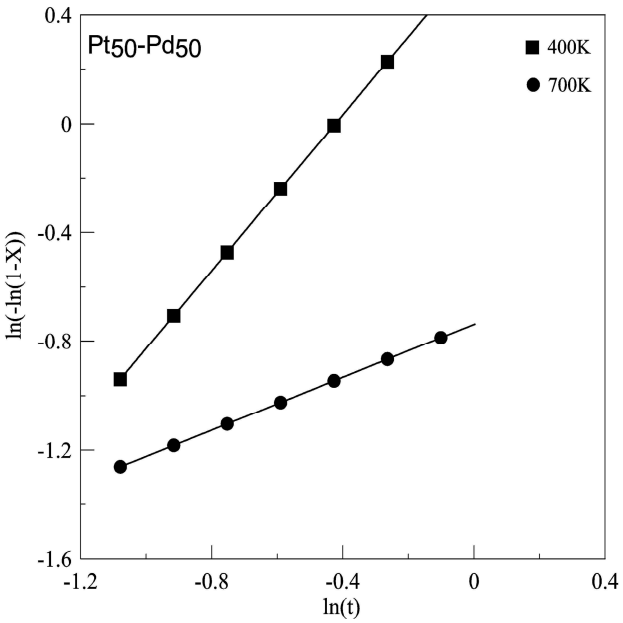

(a) Pt_{50}-Pd_{50} alloy

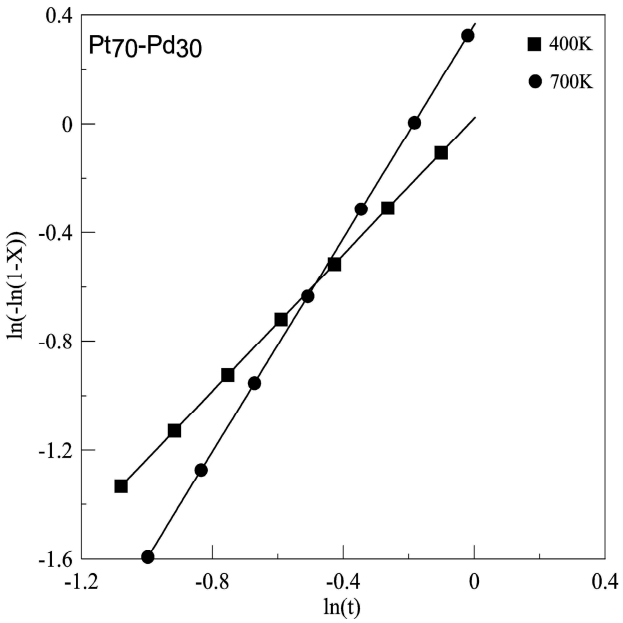

(b)Pt_{70}-Pd_{30} alloy

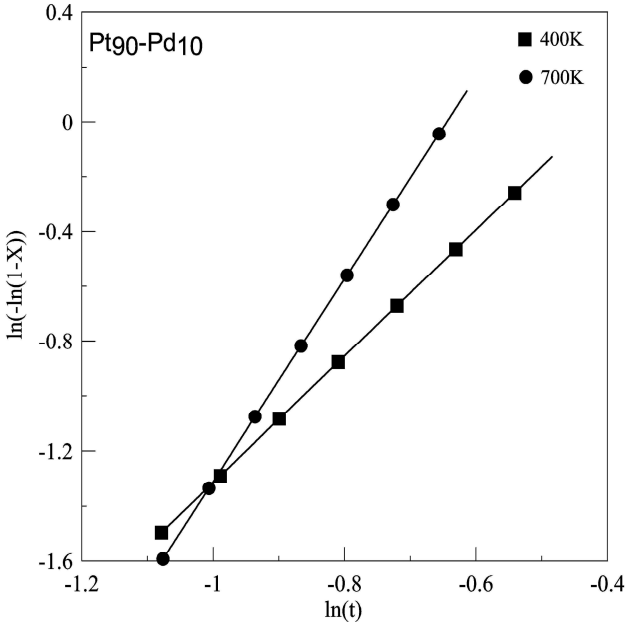

(c)Pt_{90}-Pd_{10} alloy

FIG. 5. Fitting curves of $ln(-ln(1-x))$ change with $ln(t)$ for different annealing temperatures.

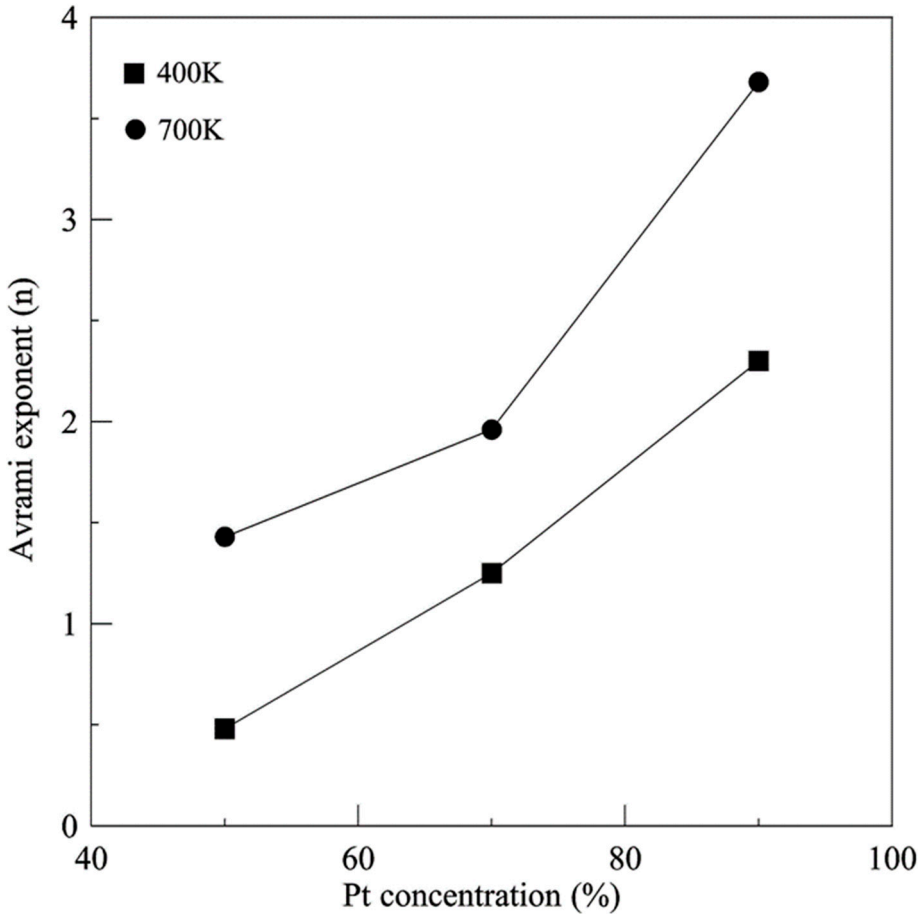

FIG. 6. The change of Avrami coefficients with Pt concentration for different annealing temperatures.

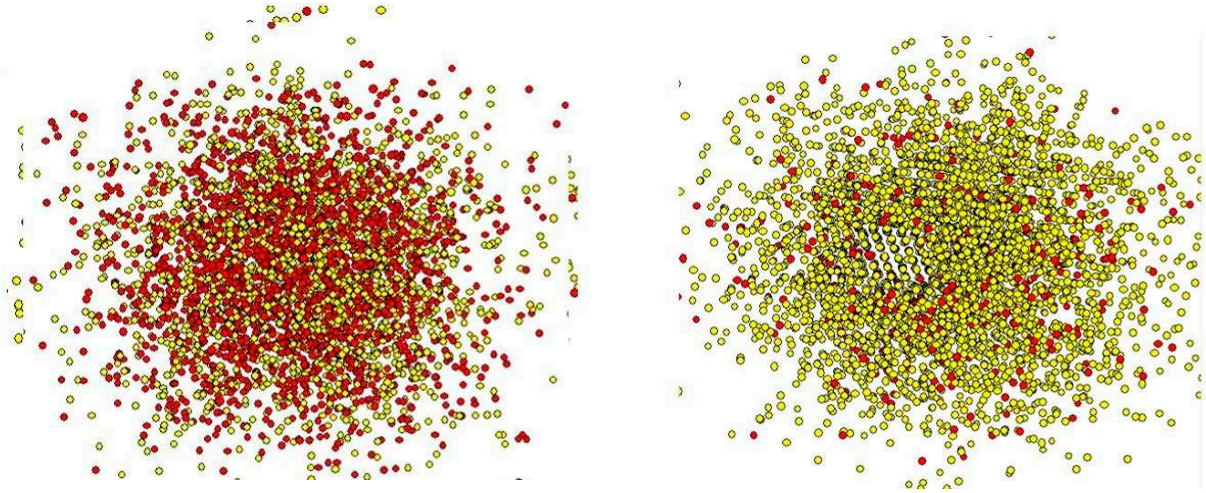

(a)Pt50-Pd50 400 K

(b)Pt_{90}-Pd_{10} 400 K

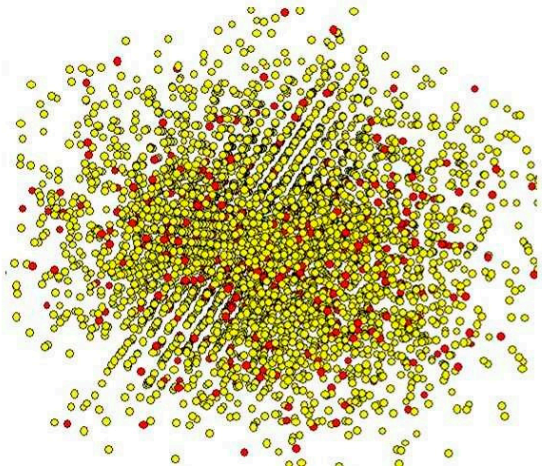

(c)Pt90-Pd10 400 K

FIG. 7. The image of atomic distribution at defined annealing temperature for alloys

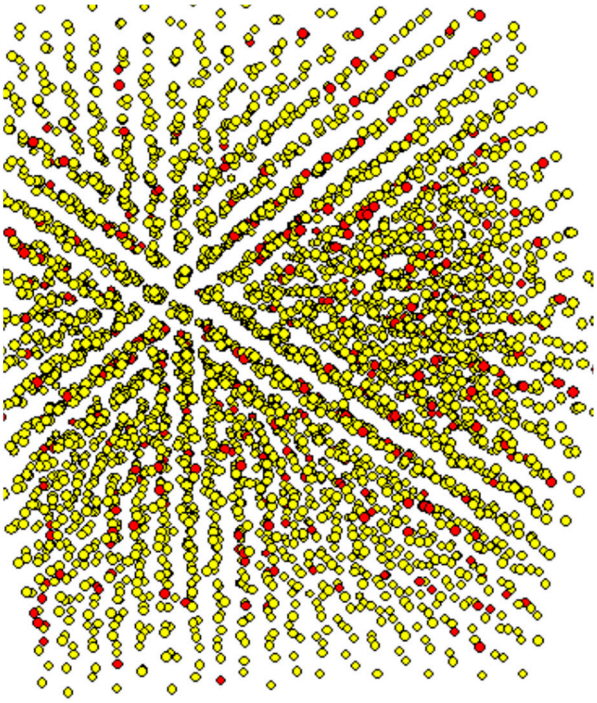

FIG. 8. The image of atomic distribution at defined annealing temperature for Pt90-Pd10 and 700 K